# A SPECTRUM PRESERVING COLLOCATION SCHEME FOR SLENDER–BODY APPROXIMATIONS TO STOKES FLOW

THOMAS GÖTZ

ABSTRACT. Linearized flows past slender bodies can be asymptotically described by a linear Fredholm integral equation. A collocation method to solve this equation is presented. In cases where the spectral representation of the integral operator is explicitly known, the collocation method recovers the spectrum of the continuous operator. The approximation error is estimated for two discretizations of the integral operator and the convergence is proved. The collocation scheme is validated in several test cases and extended to situations where the spectrum is not explicit.

## 1. INTRODUCTION

Low–Reynolds–number flows past slender fibers can be asymptotically described by a Fredholm integral equation [5,11]. Assuming a long, slender fiber with circular cross–section exposed to a free–flow one deduces from asymptotic expansions the model

(1)

$$8\pi\nu\left(\boldsymbol{u_0}(s)-\boldsymbol{u_\infty}(s)\right)=C(s)\varphi(s)+\int_0^1 \frac{\varphi(t)}{R_0}-\frac{\varphi(s)}{|s-t|}+\frac{M_0\varphi(t)}{R_0^3}-\frac{\boldsymbol{e_t}\boldsymbol{e_t}'\varphi(s)}{|s-t|}\,\mathrm{d}t,$$

where $\boldsymbol{u_0}$ is the velocity of the fiber, $\boldsymbol{u_\infty}$ is a free–stream velocity profile, $\nu>0$ the viscosity of the fluid and $s\in[0,1]$ is the normalized arc length parameter. The function $C:[0,1]\to\mathbb{R}$ is given by $C(s)=(\mathbf{I}+\boldsymbol{e_t}\boldsymbol{e_t}')\,L(s)+(\mathbf{I}-3\boldsymbol{e_t}\boldsymbol{e_t}')$. Here $\mathbf{I}$ is the identity matrix in $\mathbb{R}^3$, $\boldsymbol{e_t}\in\mathbb{R}^3$ the unit tangent vector (depending on $s$) to the fiber's centerline and $\boldsymbol{e_t}'$ its transpose; $L(s)=\ln\frac{s(1-s)}{4a^2\rho^2(s)}$ depends on the slenderness ratio $a\ll 1$ and the local radius $\rho(s)$ of the fiber. By $R_0=\|\boldsymbol{R_0}\|_2$ we denote the distance between two points $\boldsymbol{x_0}(t)$ and $\boldsymbol{x_0}(s)$ on the centerline $\boldsymbol{x_0}:[0,1]\to\mathbb{R}^3$, where $\boldsymbol{R_0}=\boldsymbol{x_0}(t)-\boldsymbol{x_0}(s)$. The matrix $M_0\in\mathbb{R}^{3\times3}$ is defined by $M_0=\boldsymbol{R_0}\boldsymbol{R_0}'$. Strictly speaking $R_0$, $\boldsymbol{R_0}$ and $\mathbf{M_0}$ depend on both $s$ and $t$. However, for the sake of shorter notation we skip this dependence henceforth. The unknown function $\varphi(s)$ equals to the force acting on the fiber.

In particular, if a straight fiber is exposed to an uniform free–flow normal to it, we obtain

$$(C+S)[\varphi]=f,\qquad\text{and}\qquad S[\varphi](s)=\int_0^1\frac{\varphi(t)-\varphi(s)}{|t-s|}\,\mathrm{d}t, \tag{2}$$

where $C(s)=\ln\left(\frac{s(1-s)}{a^2\rho^2(s)}\right)+1$ and $f=8\pi\nu\left(u_0(s)-u_\infty(s)\right)$ in the setting of (1). Considering a fiber with ellipsoidal shape, i.e. $\rho(s)=k\sqrt{s(1-s)}$ for some $k>0$, the function $C(s)$ reduces to a constant $c>0$, cf. [5].

Some of the assumptions that are met in deriving (1) can be relaxed, e.g. allowing a non–circular cross–section of the fiber [12,15]. These models are applied in various fields ranging from fiber–spinning [5,14] and biofluiddynamics [13] to the rheological

This work was supported by a grant from the DFG (Deutsche Forschungsgemeinschaft).

investigations of fiber–reinforced materials [1, 3, 4] and phase transitions of liquid crystals [17].

An extension to Oseen flow and to the description of the temperature field around a heated fiber is also possible [5]. Both Oseen's equation (for the flow–field) and the heat equation including linearized convection yield similar integral equations.

In [6, 7] a complete theory of (2) is derived. The results are based on the explicit knowledge of the spectrum of the integral operator $S$ :

$$\sigma(S) = \{-L_k \ : \ k \in \mathbb{N}_0\}\,. \tag{3}$$

Here, $L_k = \sum_{i=1}^{k} 2/i$ and by convention $L_0 = 0$. The associated eigenfunctions are the Legendre polynomials rescaled to the interval $[0, 1]$, cf. [5, 7]. This knowledge suggest an application of spectral methods to solve (2). Existence and uniqueness of solutions $\varphi$ belonging to $\mathcal{L}^2$ as well as $\mathcal{C}^1$ can be shown using the tools provided by spectral theory; for details we refer to [5, 7].

However, in the general case (1) neither the spectrum nor the eigenfunctions of the involved integral operator are available and thus spectral techniques cannot be applied. Computing the solution via successive approximations is not possible, since the integral operator is unbounded, see [5, 7]. Hence, we propose a collocation method to solve (1).

The paper is organized as follows. In Section 2 we introduce the grid used for the collocation scheme and two suitable approximations for the integral operator. These approximations use piecewise constant ansatz functions and evaluate the integral either exactly or by the midpoint quadrature yielding the discretizations $\tilde{S}_0$ and $S_0$ of the integral operator $S$. In the case of (2) the approximation error is estimated in Section 3. The approximation using the midpoint integration turns out to be of second order in the collocation points whereas the method with explicit evaluation of the integral yields an error of $\mathcal{O}(h \ln h)$. In Section 4 we prove the main result. We show, that the approximation $S_0$ conserves the spectrum of the continuous integral operator $S$. This result enables us to derive the convergence of the proposed collocation method in Section 5. Theoretically a convergence rate of $3/2$ is obtained. The collocation method is compared to the spectral method [5] in Section 6. This comparison shows quadratic convergence. In Section 7 we consider the treatment of the general equation (1) and construct a similar collocation scheme. This method is applied in Section 8 to a test case considered first by Cox [2]. The force acting on a fiber, that is bent to a circular arc, is computed.

## 2. Collocation Schemes

**Definition 1** (Collocation points)**.** Let $n \in \mathbb{N}$. By $\Gamma_n$ we define an *equidistant grid* on the interval $[0, 1]$ with a mesh width $h = 1/n$ and grid nodes $s_i = ih$ for $i = 0, \dots, n$. With this grid the cells $Z_i = [s_{i-1}, s_i)$ for $i = 1, \dots, n-1$ and $Z_n = [s_{n-1}, s_n]$ are associated.
Their midpoints are denoted by $\sigma_i = (i - 1/2)h$ for $i = 1, \dots, n$ and the set of all *collocation points* is called $\mathcal{X} = \{\sigma_i,\ i = 1, \dots, n\}$.

Let $I \subset \mathbb{R}$ denote an interval. In the following we will need the functions spaces

$$\begin{aligned}
\mathcal{B}(I) &:= \left\{ f : I \mapsto \mathbb{R} \ : \ \|f\|_\infty := \sup_{x\in I} |f(x)| \leq \infty \right\}, \\
\mathcal{C}^k(I) &:= \{ f : I \mapsto \mathbb{R} \ : \ f \text{ is } k\text{–times continuously differentiable} \}, \\
\mathcal{P}_n &:= \{ f : I \mapsto \mathbb{R} \ : \ f \text{ is a polynomial of maximal degree } n \}, \\
\mathcal{P}_n^{\text{pw}} &:= \{ f : I \mapsto \mathbb{R} \ : \ f|_{Z_i} \in \mathcal{P}_n \text{ for all grid cells } Z_i,\ i = 1, \dots, n \}.
\end{aligned}$$

**Definition 2** (Restriction and extension operator)**.** Let $\varphi \in \mathcal{B}[0,1]$. We define the *restriction operator* $R : \mathcal{B}[0,1] \mapsto \mathbb{R}^n$ by $(R[\varphi])_i := \varphi(\sigma_i)$ and $R[\varphi]$ is called the *grid function associated to* $\varphi$.
For $\boldsymbol{\psi} \in \mathbb{R}^n$ the *piecewise constant extension operator* $E_0 : \mathbb{R}^n \mapsto \mathcal{P}_0^{\mathrm{pw}}$ is defined by $(E_0[\boldsymbol{\psi}])(s) := \psi_i$ for $s \in Z_i$ and $i = 1, \dots, n$.

A grid function can be identified with a vector in $\mathbb{R}^n$. We introduce the norms

$$\|\boldsymbol{\psi}\|_p := \left( \sum_{i=1}^{n} |\psi_i|^p \right)^{1/p}, \tag{4}$$

$$\|\boldsymbol{\psi}\| := \max_{i=1,\dots,n} |\psi_i| . \tag{5}$$

**Lemma 1.** *For the restriction and the piecewise constant extension operator introduced in Definition 2 the following holds:*

$$R \circ E_0 = \mathbf{I} \qquad \textit{and} \qquad \|(E_0 \circ R)[\varphi] - \varphi\|_\infty \le h \|\varphi'\|_\infty \quad \forall \varphi \in \mathcal{C}^1[0,1].$$

*Here, we denote by* $\mathbf{I}$ *the identity matrix in* $\mathbb{R}^{n \times n}$.

In the following, integrals will often be evaluated numerically by applying the midpoint rule. We have [16, p. 171]

**Lemma 2.** *Let* $f \in \mathcal{C}^2[a,b]$*, then there exists* $\xi \in [a,b]$ *such that*

$$\int_a^b f(x)\,\mathrm{d}x = f(\tfrac{a+b}{2})(b-a) + \tfrac{(b-a)^3}{24} f''(\xi). \tag{6}$$

The basic idea of collocation methods is to replace the continuous equation (2) by a finite number of equations $(C+S)[\varphi](\sigma) = f(\sigma)$ at the collocation points $\sigma \in \mathcal{X}$. Choosing an appropriate space of ansatz functions and a suitable numerical quadrature, we can approximate the integral operator $S$ by a matrix, call it $\mathbf{S_0}$, and the multiplication operator $C$ by another matrix called $\mathbf{C}$. Hopefully, the resulting system $(\mathbf{C} + \mathbf{S_0})\boldsymbol{\psi} = R[f]$ can be solved now, yielding an approximation $\boldsymbol{\psi}$ for $\varphi$.

In the subsequent sections we will discuss two different discretizations of the integral operator $S$. Both discretizations are based on a piecewise constant approximation to the function $\varphi$.

**Definition 3.** In the situation of Definitions 1 and 2 we define the approximation

$$S_0 := E_0 \mathbf{S_0} R, \qquad \text{where} \quad (\mathbf{S_0}\boldsymbol{\psi})_j := \sum_{i \ne j} \frac{\psi_i - \psi_j}{|\sigma_i - \sigma_j|} h \tag{7}$$

or alternatively

$$\tilde{S}_0 := S E_0 R, \quad \tilde{\mathbf{S}}_\mathbf{0} = R S E_0 \qquad \text{and} \qquad \left(\tilde{\mathbf{S}}_\mathbf{0}\boldsymbol{\psi}\right)_j := \sum_{i \ne j} (\psi_i - \psi_j) \left| \ln \frac{s_i - \sigma_j}{s_{i-1} - \sigma_j} \right| . \tag{8}$$

The multiplication operator $C$ is approximated by

$$\mathbf{C}_{i,j} := C(\sigma_i)\delta_{i,j}. \tag{9}$$

Since we have chosen our collocation points $\sigma \in \mathcal{X}$ as the midpoints of the grid cells $Z$, it is quite natural to approximate the integral by the midpoint rule. This approach yields the approximation $S_0$. Plugging the piecewise constant extension of a grid function into the integral operator $S$ yields the alternative approximation $\tilde{S}_0$. In contrast to the operator $S_0$, that uses the midpoint rule for the integration, the operator $\tilde{S}_0$ performs an exact integration.

## 3. Approximation Errors

Using the approximation (7), we obtain for sufficiently smooth functions second–order accuracy in the collocation points $\sigma \in \mathcal{X}$.

**Proposition 1.** *Let $\varphi \in \mathcal{C}^3[0,1]$ and $n \in \mathbb{N}$, $h = \frac{1}{n}$. Then*

$$e_n := \|(R \circ S)[\varphi] - \mathbf{S_0}(R\varphi)\| \le K h^2, \tag{10}$$

*with a constant $K \le \|\varphi'''\|_\infty /72 + \|\varphi''\|_\infty /8$.*

*Proof.* Let $s, t \in [0,1]$. We define $\Phi_s(t) = \frac{\varphi(t)-\varphi(s)}{|t-s|}$ with the convention $\Phi_s(s) = 0$. Let $j \in \{1, \dots, n\}$. We split the integral in $S$ into the parts over $[0, s_{j-1})$, $[s_{j-1}, s_j]$ and $(s_j, 1]$. Similarly, we split the sum into the parts for $i < j$ and $i > j$. For the second integral we obtain the estimate

$$\int_{s_{j-1}}^{\sigma_j} \Phi_{\sigma_j}(t)\,\mathrm{d}t = -\int_{s_{j-1}}^{\sigma_j} \varphi'(\sigma_j) + \frac{t-\sigma_j}{2}\varphi''(\xi_{\sigma_j,-})\,\mathrm{d}t = -\left[\frac{\varphi'(\sigma_j)}{2}h - \frac{\varphi''(\xi_{\sigma_j,-})}{16}h^2\right],$$

with $\xi_{\sigma_j,-} \in [s_{j-1}, \sigma_j]$ and analogously

$$\int_{\sigma_j}^{s_j} \Phi_{\sigma_j}(t)\,\mathrm{d}t = \left[\frac{\varphi'(\sigma_j)}{2}h + \frac{\varphi''(\xi_{\sigma_j,+})}{16}h^2\right]$$

with $\xi_{\sigma_j,+} \in [\sigma_j, s_j]$. Addition yields

$$\left|\int_{s_{j-1}}^{s_j} \Phi_{\sigma_j}(t)\,\mathrm{d}t\right| = \left|\varphi''(\xi_{\sigma,-}) + \varphi''(\xi_{\sigma_j,+})\right| \frac{h^2}{16} \;\le\; \|\varphi''\|_\infty \frac{h^2}{8}.$$

For the first integral and the first summand we obtain

$$\int_0^{s_{j-1}} \Phi_{\sigma_j}(t)\,\mathrm{d}t - \sum_{i<j} \Phi_{\sigma_j}(\sigma_i) = \sum_{i<j} \Phi''_{\sigma_j}(\xi_{\sigma_j,i})\frac{h^2}{24}\left(\sigma_j - \frac{h}{2}\right),$$

and for the last integral and last summand

$$\int_{s_j}^{1} \Phi_{\sigma_j}(t)\,\mathrm{d}t - \sum_{i>j} \Phi_{\sigma_j}(\sigma_i) = \sum_{i>j} \Phi''_{\sigma_j}(\xi_{\sigma_j,i})\frac{h^2}{24}\left(1 - \sigma_j - \frac{h}{2}\right).$$

Furthermore for $\xi < s$

$$\begin{aligned}\Phi''_s(\xi) &= \frac{\varphi''(\xi)(s-\xi)^2 + 2(s-\xi)\varphi'(\xi) + 2(\varphi(\xi)-\varphi(s))}{(s-\xi)^3} \\ &= \frac{1}{(s-\xi)^3}\left[-\frac{(s-\xi)^3}{3}\varphi'''(\tilde{\xi})\right] \;=\; -\frac{\varphi'''(\tilde{\xi})}{3},\end{aligned}$$

with some $\tilde{\xi} \in (\xi, s)$. Analogously, we obtain for $\xi > s$ and $\tilde{\xi} \in (s, \xi)$, that $\Phi''_s(\xi) = \varphi'''(\tilde{\xi})/3$. Finally

$$\|(R \circ S)[\varphi] - \mathbf{S_0}(R\varphi)\| \le \left(\frac{\left\|\Phi''_{\sigma_j}\right\|_\infty}{24} + \frac{\|\varphi''\|_\infty}{8}\right) h^2 \le \left(\frac{\|\varphi'''\|_\infty}{72} + \frac{\|\varphi''\|_\infty}{8}\right) h^2.$$

Choosing $K = \|\varphi'''\|_\infty /72 + \|\varphi''\|_\infty /8$ finishes the proof. □

Now the question arises, whether this second–order is a *super–convergence* in the collocation points or if it is uniform. The term "super–convergence" expresses the well–known fact, that collocation methods can yield a higher convergence order in the collocation points than on the rest of the interval [9, pp. 133–134].

**Lemma 3.** *Let* $\varphi \in \mathcal{C}^2[0,1]$*. Then*

$$\|S[\varphi] - S_0[\varphi]\|_\infty \le Kh$$

*for some* $K > 0$*.*

*Proof.* Let $s \in Z_j$ for $j \in \{1, \dots, n\}$. Analogously to the previous proof, we split the integral into its different parts. For the integral over $Z_j$ we obtain

$$\int_{s_{j-1}}^{s_j} \Phi_s(t)\,\mathrm{d}t = \varphi'(s)\,(s_j + s_{j-1} - 2s) + \varphi''(\xi_{s,-})\frac{(s-s_{j-1})^2}{4} + \varphi''(\xi_{s,+})\frac{(s-s_j)^2}{4}$$
$$(*) \qquad \le K\,\|\varphi'\|_\infty\,h.$$

This already gives a hint on the super–convergence of the piecewise constant approximation for cell–centered collocation. Considering the remaining part of the integral, one deduces for the first part

$$\begin{aligned}\int_0^{s_{j-1}} \Phi_s(t)\,\mathrm{d}t - \sum_{i<j} \Phi_{\sigma_j}(\sigma_i)h &= \sum_{i<j} \int_{s_{i-1}}^{s_i} \Phi_s(t) - \Phi_{\sigma_j}(\sigma_i)\,\mathrm{d}t \\ &= \sum_{i<j} h\left[\Phi_s(\xi_i) - \Phi_{\sigma_j}(\sigma_i)\right] \\ &\le \sum_{i<j} h^2\,\|\varphi''\|_\infty\,,\end{aligned}$$

and a similar result for the integral from $s_j$ to 1, resp. the sum over $i > j$. Including $(*)$ yields

$$\left|\int_0^1 \Phi_s(t)\,\mathrm{d}t - \sum_{i\ne j} \Phi_{\sigma_j}(\sigma_i)h\right| \le \sum_{i\ne j} h^2\,\|\varphi''\|_\infty + Kh\,\|\varphi'\|_\infty \;\le\; hK.$$

Thus, we obtain only first–order convergence for $s \in Z_j$. □

Concerning the alternative approximation $\tilde{S}_0$, one might expect a better approximation, since the integration is performed exact rather than using the midpoint rule. The next proposition states the rather surprising result, that this is not the case.

**Proposition 2.** *Let* $\varphi \in \mathcal{C}^2[0,1]$*. The discretization with analytic calculation of the integrals, i.e. the operator* $\tilde{\mathbf{S}}_\mathbf{0}$*, approximates the integral operator* $S$ *with an error bounded by the estimate*

$$\tilde{e}_n := \left\|(R \circ S)[\varphi] - \tilde{\mathbf{S}}_\mathbf{0}(R\varphi)\right\| \le Kh \ln\frac{1}{h},$$

*where* $K > 0$ *is some constant.*

*Proof.* Analogously to the proof of Proposition 1, we fix a collocation point $\sigma_j \in \mathcal{X}$ and split the integral into the part over $Z_j$ and the rest. For the integration over $Z_j$

$$(*) \qquad \left|\int_{Z_j} \Phi_{\sigma_j}(t)\,\mathrm{d}t\right| \le \|\varphi''\|_\infty \frac{h^2}{8}$$

holds, using the notations from the proof of Proposition 1.
For the remaining integration we use

$$|\varphi(t) - \varphi(\sigma_i)| \le \|\varphi'\|_\infty \frac{h}{2},$$

| $\varphi(s)$ | Approximation $\mathbf{S_0}$ | | | |
|---|---|---|---|---|
| | $n=50$ | $n=100$ | $n=200$ | $\gamma$ |
| $s^3$ | 2.64 E-4 | 6.64 E-5 | 1.66 E-5 | 2.00 |
| $s^2$ | 1.00 E-4 | 2.50 E-5 | 6.25 E-6 | 2.00 |
| $s^1$ | 1.53 E-15 | 3.33 E-15 | 5.11 E-15 | |
| 1 | 3.48 E-15 | 7.91 E-15 | 1.14 E-14 | |

| $\varphi(s)$ | Approximation $\tilde{\mathbf{S}}_\mathbf{0}$ | | | |
|---|---|---|---|---|
| | $n=50$ | $n=100$ | $n=200$ | $\tilde{\gamma}$ |
| $s^3$ | 8.76 E-3 | 4.47 E-3 | 2.26 E-3 | 0.98 |
| $s^2$ | 5.96 E-3 | 3.02 E-3 | 1.52 E-3 | 0.99 |
| $s^1$ | 3.03 E-3 | 1.53 E-3 | 7.63 E-4 | 1.00 |
| 1 | 1.37 E-15 | 2.04 E-15 | 2.73 E-15 | |

TABLE 1. Absolute error and convergence rates in the collocation points for the test cases (11) using the approximations $\mathbf{S_0}$ (7) and $\tilde{\mathbf{S}}_\mathbf{0}$ (8).

where $t \in Z_i$ and obtain

$$\left| \sum_{i \neq j} \int_{Z_i} \frac{\varphi(t) - \varphi(\sigma_i)}{|t - \sigma_j|} \, \mathrm{d}t \right| \leq \|\varphi'\|_\infty \frac{h}{2} \ln \frac{\sigma_j(1-\sigma_j)}{h^2/4} \leq \|\varphi'\|_\infty \, h \ln \frac{1}{h},$$

which dominates the error $(*)$. □

Similar to Lemma 3 one can show, that the operator $\tilde{S}_0$ approximates the operator $S$ up to first order on the whole interval $[0, 1]$.

Table 1 shows the results for the approximations $\mathbf{S_0}$ and $\tilde{\mathbf{S}}_\mathbf{0}$ using the test cases

$$S[\varphi](s) = -L_n s^n + \sum_{k=0}^{n-1} \frac{1}{n-k} s^k \qquad \text{for} \quad \varphi(s) = s^n, \tag{11}$$

where $-L_n = -\sum_{k=1}^{n} \frac{2}{k}$ for $n \in \mathbb{N}_0$ are the eigenvalues of $S$, see [7] or Equation (3). By convention we have $L_0 = 0$.

The errors $e_n$ and $\tilde{e}_n$ are defined in the Propositions 1 and 2. The *numerical convergence order* $\gamma$ or $\tilde{\gamma}$ is defined as

$$\gamma_n := \log_2 \frac{e_{n/2}}{e_n} \quad \text{resp.} \quad \tilde{\gamma}_n := \log_2 \frac{\tilde{e}_{n/2}}{\tilde{e}_n}$$

where $\log_2$ denotes the logarithm with respect to base 2. The expected $\mathcal{O}(h^2)$–error in the collocation points for the midpoint rule (operator $\mathbf{S_0}$) is clearly visible as well as the almost linear convergence for the method with exact calculation of the integrals (operator $\tilde{\mathbf{S}}_\mathbf{0}$). For $\varphi(s) = 1$ and $\varphi(s) = s$ the midpoint rule is exact up to machine precision, whereas the other method is only exact for the trivial constant case.

## 4. Spectral Properties

The discrete spectrum and the associated eigenfunctions of the continuous operator $S$ are explicitly known. An interesting property of the midpoint–discretization $\mathbf{S_0}$ is, that it recovers the spectrum of $S$.

We need a preliminary result.

**Lemma 4.** *Let $n, k \in \mathbb{N}_0$. Then*

$$\sum_{j=1}^{n}(2j-1)^k = \frac{2^k n^{k+1}}{k+1} - \sum_{\mu=1}^{\lfloor k/2\rfloor} C_{\mu,k} n^{k+1-2\mu},$$

*where $\lfloor r\rfloor := \max_{n\in\mathbb{N}_0}\{n \le r\}$ denotes the Gauss–bracket,*
*$C_{\mu,k} = \frac{B_{2\mu}}{2\mu}2^{k+1-2\mu}\left(2^{2\mu-1}-1\right)\binom{k}{2\mu-1}$ and $B_n$ are the Bernoulli–numbers, see [8, Formula 0.122].*

**Theorem 1.** *The spectrum of the finite–dimensional approximation $\mathbf{S_0}$ to the integral operator $S$ is given by*

$$\sigma(\mathbf{S_0}) = \{-L_k,\ k=0,\dots,n-1\}. \tag{12}$$

*Proof.* Let $\boldsymbol{s} = \left(\frac{i-1/2}{n}\right)_{i=1,\dots,n} \in \mathbb{R}^n$ and $\boldsymbol{s^l} = \left(s_i^l\right)_{i=1,\dots,n}$ for $l=0,\dots,n-1$.
Then $\left\{\boldsymbol{s^0},\dots,\boldsymbol{s^{n-1}}\right\}$ is a basis of $\mathbb{R}^n$, since the matrix with columns $\left(\boldsymbol{s^l}\right)_{l=0,\dots,n-1}$ is a Vandermonde–matrix.
Obviously, $\boldsymbol{s^0} \in \ker \mathbf{S_0}$.
Next, we show that for $l \in \{1,\dots,n-1\}$ we have $\mathbf{S_0}\boldsymbol{s^l} = -L_l\boldsymbol{s^l} + \boldsymbol{p_{l-1}}$, where $\boldsymbol{p_{l-1}} \in \operatorname{span}\{\boldsymbol{s^0},\dots,\boldsymbol{s^{l-1}}\}$. Define $i' = i-1/2$ and $j' = j-1/2$. Then

$$
\begin{aligned}
(\mathbf{S_0}\boldsymbol{s^l})_i &= \frac{1}{n^l}\sum_{i\neq j}\frac{(j-\frac12)^l-(i-\frac12)^l}{|j-i|}\\
&= \frac{1}{n^l}\left(\sum_{j=1}^{n} + \delta_{i,j} - 2\sum_{j=1}^{i}\right)\left(\sum_{k=0}^{l-1} {i'}^{l-k-1}{j'}^{k}\right)\\
&= \frac{l(i')^{l-1}}{n^l} - \frac{2}{n^l 2^{l-1}}\sum_{k=0}^{l-1}(2i')^{l-k-1}\sum_{j=1}^{i}(2j-1)^k + \frac{1}{n^l 2^{l-1}}\sum_{k=0}^{l-1}(2i')^{l-k-1}\sum_{j=1}^{n}(2j-1)^k\\
&= \frac{l(i')^{l-1}}{n^l} - \frac{2}{n^l 2^l}\sum_{k=0}^{l-1}(2i')^{l-k-1}\left(\frac{(2i)^{k+1}}{k+1} - \sum_{\mu} 2C_{\mu,k} i^{k+1-2\mu}\right)\\
&\qquad + \frac{1}{n^l 2^l}\sum_{k=0}^{l-1}(2i')^{l-k-1}\left(\frac{(2n)^{k+1}}{k+1} - \sum_{\mu} 2C_{\mu,k} n^{k+1-2\mu}\right)\\
&= \frac{l(i')^{l-1}}{n^l} - \frac{2}{n^l 2^l}\sum_{k=0}^{l-1}(2i')^{l-k-1}\left[\frac{(2i)^{k+1}}{k+1} + \frac{1}{k+1}\sum_{m=1}^{k+1}\binom{k+1}{m}(-1)^m(2i)^{k+1-m}\right.\\
&\qquad\qquad \left. - \frac{1}{k+1}\sum_{m=1}^{k+1}\binom{k+1}{m}(-1)^m(2i)^{k+1-m} - \sum_{\mu} 2C_{\mu,k} i^{k+1-2\mu}\right]\\
&\qquad + \frac{1}{n^l 2^l}\sum_{k=0}^{l-1}(2i')^{l-k-1}\left(\frac{(2n)^{k+1}}{k+1} - \sum_{\mu} 2C_{\mu,k} n^{k+1-2\mu}\right)\\
&= \frac{l(i')^{l-1}}{n^l} \underbrace{- \frac{2}{n^l 2^l}\left[(2i')^l\sum_{k=0}^{l-1}\frac{1}{k+1}\right.}_{(*)} - \sum_{k=0}^{l-1}(2i')^{l-k-1} \times\\
&\qquad\qquad \left.\times\left(\frac{1}{k+1}\sum_{m=1}^{k+1}\binom{k+1}{m}(-1)^m(2i)^{k+1-m} + \sum_{\mu} 2C_{\mu,k} i^{k+1-2\mu}\right)\right]\\
&\qquad + \frac{1}{n^l 2^l}\sum_{k=0}^{l-1}(2i')^{l-k-1}\left(\frac{(2n)^{k+1}}{k+1} - \sum_{\mu} 2C_{\mu,k} n^{k+1-2\mu}\right)
\end{aligned}
$$

$$= -L_l \boldsymbol{s^l} + \boldsymbol{p_{l-1}}.$$

Note, that the term $(*)$ is the only term that contains the vector $\boldsymbol{s^l}$. All the other terms are linear combinations of the vectors $\boldsymbol{s^0}, \ldots, \boldsymbol{s^{l-1}}$. Thus, writing $\mathbf{S_0}$ in the basis $\left\{\boldsymbol{s^k}\right\}_{k=0,\ldots,n-1}$, we obtain the following upper diagonal form

$$\mathbf{S_0} = \begin{bmatrix} 0 & * & \cdots & * \\ 0 & -L_1 & \cdots & * \\ \vdots & \vdots & \ddots & \vdots \\ 0 & 0 & \cdots & -L_{n-1} \end{bmatrix},$$

where the entries marked by $*$ correspond to the representation of $\boldsymbol{p_{l-1}}$ with respect to the basis $\left\{\boldsymbol{s^k}\right\}_{k=0,\ldots,n-1}$. The eigenvalues of this upper triangular matrix are the entries along the diagonal. □

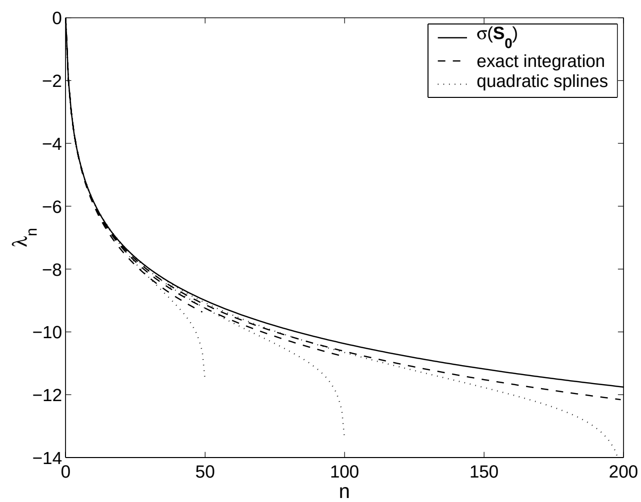


FIGURE 1. The spectra of the matrices $\mathbf{S_0}$ ('—'), $\tilde{\mathbf{S}}_\mathbf{0}$ ('– –') and from a collocation scheme based on quadratic splines ('$\cdots$') are plotted. The spectrum of $\mathbf{S_0}$ is identical to the spectrum of the integral operator $S$, see Theorem 1. The two other spectra are computed numerically for different discretizations yielding matrices of size $n \times n$, where $n \in \{50, 100, 200\}$. The differences in the spectra are significant, especially for the collocation based on spline–approximation.

*Remark* 1. Theorem 1 as well as its proof are the discrete analogon of a similar result in the continuous case [7]. The basis vectors $\boldsymbol{s^l}$ are, so to speak, *discrete monomials* and $\boldsymbol{p} \in \text{span}\left\{\boldsymbol{s^l}, l = 0, \ldots, k \text{ for } k \le n-1\right\}$ might be called a *discrete polynomial of degree* $k$, if $\boldsymbol{p}\boldsymbol{s^k} \neq 0$. The statement of Theorem 1 can be reformulated as :

$$\mathbf{S_0}\left[\text{span}\left\{\boldsymbol{s^l}, l = 0, \ldots, k\right\}\right] = \text{span}\left\{\boldsymbol{s^l}, l = 0, \ldots, k\right\}$$

for all $k \le n-1$. The matrix $\mathbf{S_0}$ maps discrete polynomials onto discrete polynomials.

Using Gram–Schmidt orthogonalization, we can construct a basis $\{\boldsymbol{u_0}, \ldots, \boldsymbol{u_{n-1}}\}$ of eigenvectors that diagonalizes $\mathbf{S_0}$.

1. Define $\boldsymbol{u_0} := \boldsymbol{s^0}$. Then $\mathbf{S_0}\boldsymbol{u_0} = -L_0\boldsymbol{u_0}$.
2. Define $\boldsymbol{u_k} := \boldsymbol{s^k} + \sum_{j=0}^{k-1} r_{k-1}^j \boldsymbol{u_j}$, where $r_{k-1}^j = -p_{k-1}^j/(L_k - L_j)$ and $\boldsymbol{p_{k-1}} = \sum_{j=0}^{k-1} p_{k-1}^j \boldsymbol{u_j}$.

The resulting sequence $(\boldsymbol{u_k})_{k=0,\dots,n-1}$ is a basis of eigenvectors, that diagonalizes $\mathbf{S_0}$.

From the theoretical investigation of $S$ performed in [5,7] we know, that there exist eigenfunctions $\tilde{P}_k \in \mathcal{P}_k$ such that $S[\tilde{P}_k] = -L_k\tilde{P}_k$ and $\tilde{P}_k = s^k + \sum_{j=0}^{k-1} w_{k-1}^j \tilde{P}_j$. Furthermore $S[s^k] = -L_k s^k + q_{k-1}(s)$ where $q_{k-1} \in \mathcal{P}_{k-1}$. Now the question arises, whether the *numerical* eigenvectors $\boldsymbol{u_k}$ of $\mathbf{S_0}$ converge for fixed $k$ and $h \to 0$ to the eigenfunctions $\tilde{P}_k$ of the operator $S$.
The following Lemma 5 and Proposition 3 give the affirmative answer to this question.

**Lemma 5.** *Let $k \in \mathbb{N}_0$ and $n > k$. Then*

$$\|\boldsymbol{p_{k-1}} - R[q_{k-1}]\| \le \frac{k(k-1)}{8}\left(1 + \frac{k-2}{9}\right)h^2,$$

*for grid size $h \to 0$.*

*Proof.* Recall, that $\mathbf{S_0}\boldsymbol{s^k} = -L_k\boldsymbol{s^k} + \boldsymbol{p_{k-1}}$ and $(R \circ S)[s^k] = -L_k R[s^k] + R[q_{k-1}]$. Thus

$$\|\boldsymbol{p_{k-1}} - R[q_{k-1}]\| \le \left\|\mathbf{S_0}\boldsymbol{s^k} - (R \circ S)[s^k]\right\| \le K h^2$$

where

$$K \le \frac{\left\|(s^k)'''\right\|_\infty}{72} + \frac{\left\|(s^k)''\right\|_\infty}{8} \le \frac{k(k-1)(k-2)}{72} + \frac{k(k-1)}{8}.$$

□

**Proposition 3.** *Let $k \in \mathbb{N}_0$ and $n > k$. Then*

$$\left\|\boldsymbol{u_k} - R[\tilde{P}_k]\right\| \le \frac{k(k-1)}{8}\left(1 + \frac{k-2}{9}\right)h^2 \sum_{j=0}^{k-1} \frac{1}{L_k - L_j}.$$

*Proof.* Using the results $\boldsymbol{u_k} = \boldsymbol{s^k} + \sum_{j=0}^{k-1} r_{k-1}^j \boldsymbol{u_j}$ and $r_{k-1}^j = -\frac{p_{k-1}^j}{L_k - L_j}$ as well as $\boldsymbol{p_{k-1}} = \sum_{j=0}^{k-1} p_{k-1}^j \boldsymbol{u_j}$, we obtain the estimate

$$\begin{aligned}\left\|\boldsymbol{u_k} - R[\tilde{P}_k]\right\| &\le \sum_{j=0}^{k-1}\left\|r_{k-1}^j \boldsymbol{u_j} - w_{k-1}^j R[\tilde{P}_j]\right\| \le \sum_{j=0}^{k-1} \frac{\left\|p_{k-1}^j \boldsymbol{u_j} - q_{k-1}^j R[\tilde{P}_j]\right\|}{L_k - L_j} \\ &\le \sum_{j=0}^{k-1} \frac{\|\boldsymbol{p_{k-1}} - R[q_{k-1}]\|}{L_k - L_j}\end{aligned}$$

and finally by Lemma 5

$$\left\|\boldsymbol{u_k} - R[\tilde{P}_k]\right\| \le \frac{k(k-1)}{8}\left(1 + \frac{k-2}{9}\right)h^2 \sum_{j=0}^{k-1} \frac{1}{L_k - L_j}.$$

□

As a summary :
*The numerical discretization $\mathbf{S_0}$ exactly reproduces the spectrum of the continuous operator. The eigenvectors of the numerical scheme converge to the eigenfunctions of the continuous operator.*

## 5. Convergence

We will exploit the spectral properties of $\mathbf{S_0}$ and of $S$ to derive convergence results for a numerical scheme.

The continuous equation

$$(C+S)[\varphi] = f, \qquad \text{where} \qquad S[\varphi](s) = \int_0^1 \frac{\varphi(t)-\varphi(s)}{|t-s|}\,\mathrm{d}t \tag{13}$$

is replaced by the numerically solvable equation

$$(\mathbf{C}+\mathbf{S_0})\boldsymbol{\psi} = \boldsymbol{f}, \tag{14}$$

where $\boldsymbol{f} = R[f]$ is the grid function associated to $f$.

**Theorem 2.** *Let $C = c = const.$ and $c \neq L_k$ for $k \in \mathbb{N}_0$. Let $\varphi$ be the solution of* (13)*. Let $\boldsymbol{\psi}$ be the solution of the discrete equation* (14) *and by $\boldsymbol{e} = R[\varphi] - \boldsymbol{\psi}$ we denote the error. Then there exists $K > 0$, such that*

$$\|\boldsymbol{e}\| \leq K h^{3/2}.$$

*Proof.* In a collocation point $\sigma_i \in \mathcal{X}$ we obtain

$$(C+S)\,[\varphi](\sigma_i) = \sum_{j=1}^n (\mathbf{C}+\mathbf{S_0})_{i,j}\,\boldsymbol{\psi}_j.$$

Since $C$ is a multiplication operator and according to Definition 3, the matrix $\mathbf{C}$ is a diagonal matrix. Hence $C[\varphi](\sigma_i) = C(\sigma_i)\,\varphi(\sigma_i) = \sum_{j=1}^n \mathbf{C}_{i,j}(R\varphi)_j$. Setting $\mathbf{M} = \mathbf{C}+\mathbf{S_0}$ yields

$$\sum_j \mathbf{M}_{i,j}\boldsymbol{e}_j = \mathbf{S_0}(R[\varphi]) - (R\circ S)[\varphi].$$

The eigenvalues of $\mathbf{M}$ are given by $\{c - L_k \,:\, k = 0,\dots,n-1\}$. Due to our assumption $c \neq L_k$ for $k \in \mathbb{N}_0$ the matrix $\mathbf{M}$ is invertible and

$$\boldsymbol{e}_i = \sum_j \mathbf{M}^{-1}_{i,j}\left(\mathbf{S_0}(R[\varphi]) - (R\circ S)[\varphi]\right)_j.$$

Thus we obtain the estimate

$$\|\boldsymbol{e}\| \leq \left\|\mathbf{M}^{-1}\right\|_\infty \cdot \|(R\circ S)[\varphi] - \mathbf{S_0}(R[\varphi])\|.$$

The second factor is bounded by $Kh^2$ for some $K > 0$ due to Proposition 1. Considering the first term, let $\rho(\mathbf{M})$ denote the spectral radius and $\lambda_{\min}(\mathbf{M})$ be the eigenvalue of $\mathbf{M}$ with minimal absolute value. We have

$$\|\mathbf{M}\|_\infty \leq \sqrt{n}\,\rho(\mathbf{M}).$$

For $\|\mathbf{M}^{-1}\|_\infty$ we obtain

$$\|\mathbf{M}^{-1}\|_\infty \leq \sqrt{n}\,\rho(\mathbf{M}^{-1}) \leq \sqrt{n}\,\lambda_{\min}(\mathbf{M})^{-1}.$$

Since $C = c = \text{const.}$, the smallest eigenvalue of $\mathbf{M}$ is given by

$$\lambda_{\min}(\mathbf{M}) = \min_{\lambda\in\sigma(\mathbf{S_0})} |c+\lambda|.$$

If $n$ is large enough, i.e. if $c - L_n < 0$, this term is independent of $n$ and bounded by some constant $K > 0$. Summarizing the results, we obtain

$$\|\boldsymbol{e}\| \leq K\sqrt{n}h^2 = Kh^{3/2}$$

□

Thus we have a convergence rate of at least 3/2. The numerical results given in Table 2 exhibit a convergence rate of approximately 2. So there might be some space for slight improvements.

What about the case $C \neq$ const. ? Until now, we used in deriving lower bounds for the eigenvalues of $\mathbf{M}$, that $C(s) = c =$ const..
In the case of non–constant $C$, we use a perturbation argument, reducing the case of non–constant $C$ to the situation for $C =$ const.

**Lemma 6.** *Let $\mathbf{A} \in \mathbb{R}^{n\times n}$ be regular and $\mathbf{E} \in \mathbb{R}^{n\times n}$ be a perturbation, such that $\|\mathbf{A^{-1}}\| \cdot \|\mathbf{E}\| \leq 1$. Then $\mathbf{A}+\mathbf{E}$ is again regular and the estimate*

$$\|(\mathbf{A}+\mathbf{E})^{-1}\| \leq \frac{\|\mathbf{A^{-1}}\|}{1-\|\mathbf{A^{-1}}\|\cdot\|\mathbf{E}\|}.$$

*holds in any matrix–norm $\|\cdot\|$, see [16, p. 63].*

If $C \neq$ const., we define $c = \frac{1}{n}\sum_{i=0}^{n-1}(\boldsymbol{R}C)_i$, $\mathbf{\Delta} = \mathbf{C} - c\mathbf{I}$ $\mathbf{M} = \mathbf{C} + \mathbf{S_0}$ and $\hat{\mathbf{M}} = c\mathbf{I} + \mathbf{S_0}$.

**Corollary 1.** *If $\|\hat{\mathbf{M}}^{\mathbf{-1}}\| \cdot \|\mathbf{\Delta}\| \leq 1$, then due to Lemma 6*

$$\|\mathbf{M^{-1}}\| \leq \frac{\|\hat{\mathbf{M}}^{\mathbf{-1}}\|}{1-\|\hat{\mathbf{M}}^{\mathbf{-1}}\|\cdot\|\mathbf{\Delta}\|}$$

*holds. Especially*

$$\|\mathbf{M}^{-1}\|_\infty \leq \frac{\sqrt{n}}{\lambda_{\min}(\hat{\mathbf{M}}) - \max\limits_{i=0,\ldots,n-1}|C_i - c|)}.$$

*Remark* 2. The result of Corollary 1 restricts to the case

$$\max_{i=0,\ldots,n-1}|C_i - c| \leq \lambda_{\min}(\hat{\mathbf{M}}) = \min_{k\in\mathbb{N}_0}|c - L_{k-1}|.$$

For example, if $c = 5$, then we have $\min_{k\in\mathbb{N}_0}|c - L_{k-1}| = 0.1$ and for $c = 14$ even $\min_{k\in\mathbb{N}_0}|c - L_{k-1}| \approx 6.986\cdot 10^{-4}$ for $k = 615$.

## 6. Numerical Results

We compare the collocation method with a spectral method proposed in [7]. The right hand side of (2) is given by the functions

$$f(s) := -\sin(2\pi s)$$
$$h_\delta(s) := \frac{1}{\pi}\arctan\left(\frac{2s-1}{\delta}\right) + \frac{1}{2}.$$

The Legendre coefficients of the reference solution are obtained using `MAPLE V Release 4`. The expansion in the Legendre polynomial basis is cut off with a $\mathcal{L}^2$–error less than $10^{-5}$. For the function $f(s) = -\sin(2\pi s)$ the first 11 coefficients guarantee a $\mathcal{L}^2$–approximation with an error of approximately $8.4\cdot 10^{-6}$. For $h_\delta(s) = \frac{1}{\pi}\arctan(\frac{2s-1}{\delta}) + \frac{1}{2}$ with $\delta = 5$ the first 39 coefficients are needed and yield a $\mathcal{L}^2$–error of about $7.8\cdot 10^{-6}$. Again, the parameter $c = 5$ is chosen. With this choice, the solution is computed with $\mathcal{L}^2$–error less than $10^{-5}$.

The collocation method uses 50 up to 400 collocation points, i.e. the mesh width is between $h = 0.02$ and $0.0025$. The computation of the solution requires the inversion of a full but symmetric matrix of dimension $n \times n$.

Table 2 lists the errors between the reference solution and the numerical ones in the $\mathcal{L}^\infty$– and $\mathcal{L}^2$–norm (both normalized with the $\mathcal{L}^\infty$– resp. $\mathcal{L}^2$–norm of the reference solution). For the error $e_\infty$ the numerical convergence order $\gamma$ is also given.

TABLE 2. $\mathcal{L}^\infty$–error $e_\infty$ along with the convergence order $\gamma$ and $\mathcal{L}^2$–error $e_2$ for $f(s)$ and $h_{1/5}(s)$.

| $n =$ | Test case $f$ | | | Test case $h_{1/5}$ | | |
|---|---|---|---|---|---|---|
| | $e_\infty$ | $\gamma$ | $e_2$ | $e_\infty$ | $\gamma$ | $e_2$ |
| 50 | 1.3225 E-2 | | 1.8765 E-3 | 2.9890 E-2 | | 9.8854 E-4 |
| 100 | 3.6285 E-3 | 1.87 | 4.6120 E-4 | 8.5338 E-3 | 1.81 | 2.3864 E-4 |
| 200 | 9.5020 E-4 | 1.93 | 1.0672 E-4 | 2.2858 E-3 | 1.90 | 5.1680 E-5 |
| 400 | 2.4409 E-4 | 1.96 | 1.8061 E-5 | 5.9209 E-4 | 1.95 | 4.9725 E-6 |

TABLE 3. $\mathcal{L}^\infty$–error $\tilde{e}_\infty$ along with the convergence order $\tilde{\gamma}$ and $\mathcal{L}^2$–error $\tilde{e}_2$ for $f(s)$ and $h_{1/5}(s)$ using the alternative approximation $\tilde{S}_0$.

| $n =$ | Test case $f$ | | | Test case $h_{1/5}$ | | |
|---|---|---|---|---|---|---|
| | $\tilde{e}_\infty$ | $\tilde{\gamma}$ | $\tilde{e}_2$ | $\tilde{e}_\infty$ | $\tilde{\gamma}$ | $\tilde{e}_2$ |
| 50 | 3.1178 E-2 | | 6.7005 E-3 | 6.9975 E-2 | | 3.4469 E-2 |
| 100 | 1.9763 E-2 | 0.65 | 2.0394 E-3 | 4.3879 E-2 | 0.67 | 1.8684 E-2 |
| 200 | 1.1858 E-2 | 0.74 | 6.0923 E-4 | 2.5837 E-2 | 0.76 | 7.5078 E-3 |
| 400 | 5.4897 E-3 | 1.11 | 1.8528 E-4 | 1.1865 E-2 | 1.12 | 2.5611 E-2 |

This table shows nearly quadratic numerical convergence rates for the collocation scheme.

Table 3 shows the analogous result for the alternative approximation $\tilde{S}_0$ to the integral operator $S$.

## 7. NUMERICAL TREATMENT OF THE GENERAL EQUATION

The considerations up to now are concerned with a straight fiber exposed to normal or tangential flow, i.e. Equation (2). In this section we briefly discuss the numerical treatment of Equation (1) rewritten as

(15)
$$\boldsymbol{f}(s) = (C_1(s)\mathbf{I} + C_2(s)\boldsymbol{e_t}\boldsymbol{e_t}')\,\boldsymbol{\varphi}(s) + \int_0^1 \frac{\boldsymbol{\varphi}(t)}{R_0} - \frac{\boldsymbol{\varphi}(s)}{|s-t|} + \frac{\mathbf{M_0}\boldsymbol{\varphi}(t)}{R_0^3} - \frac{\boldsymbol{e_t}\boldsymbol{e_t}'\boldsymbol{\varphi}(s)}{|s-t|}\,\mathrm{d}t.$$

First, we note, that for a $\mathcal{C}^2$–function $\boldsymbol{x_0}$ describing the centerline of the fiber, we obtain

$$R_0 = \|\boldsymbol{x_0}(s) - \boldsymbol{x_0}(t)\| = |s-t| + \frac{\kappa}{2}|s-t|^2 + \mathcal{O}(|s-t|^3) \qquad \text{for } t \to s,$$

as well as

$$\frac{\mathbf{M_0}}{R_0^2} = \left(\frac{\boldsymbol{R_0}}{R_0}\right)\left(\frac{\boldsymbol{R_0}}{R_0}\right)' = \boldsymbol{e_t}\boldsymbol{e_t}' + \frac{\kappa}{2}|s-t|\,\boldsymbol{e_t}\otimes\boldsymbol{e_n} + \mathcal{O}(|s-t|^2) \quad \text{for } t \to s,$$

where $\kappa$ is the curvature of the centerline and $\boldsymbol{a}\otimes\boldsymbol{b} := \boldsymbol{a}\boldsymbol{b}' + \boldsymbol{b}\boldsymbol{a}'$ is the symmetrized dyadic product of $\boldsymbol{a}, \boldsymbol{b} \in \mathbb{R}^3$. The integral of (15) exists for $\alpha$–Hölder–continuous functions $\boldsymbol{\varphi} \in \mathcal{C}^{0,\alpha}[0,1]$ where $\alpha \in (0,1]$, i.e. for $t \to s$, the integrand of (15) "reduces" to that of (13). For $t$ "away" from $s$, the integrand of (15) reflects the shape of the fiber's centerline. If the centerline of the fiber does not reapproach itself, i.e. if $\|\boldsymbol{x_0}(t) - \boldsymbol{x_0}(s)\| \geq K|s-t|$, then the terms containing $R_0^{-1}$ and $R_0^{-3}$ in (15) cannot have singularities for $t \neq s$.

As already stated, an explicit spectral theory of (15) is presently not available. Nevertheless, since the collocation method using piecewise constant ansatz functions and midpoint integration works well in the case of (2), we construct a similar method for solving (15).

Rewriting (15) componentwise with respect to the global coordinate system in $\mathbb{R}^3$, we obtain a system of three coupled integral equations for the components $(\varphi_1, \varphi_2, \varphi_3) = \boldsymbol{\varphi}$. Using a piecewise constant ansatz for each component and discretizing the integrals with the midpoint quadrature formula, we obtain after some calculations a linear system $\left(\mathbf{C} + \mathbf{S}_\mathbf{0}^{\text{full}}\right) \boldsymbol{\varphi} = \boldsymbol{f}$,

$$\begin{pmatrix} \mathbf{S}_\mathbf{0}^{\mathbf{11}} & \mathbf{S}_\mathbf{0}^{\mathbf{12}} & \mathbf{S}_\mathbf{0}^{\mathbf{13}} \\ \mathbf{S}_\mathbf{0}^{\mathbf{21}} & \mathbf{S}_\mathbf{0}^{\mathbf{22}} & \mathbf{S}_\mathbf{0}^{\mathbf{23}} \\ \mathbf{S}_\mathbf{0}^{\mathbf{31}} & \mathbf{S}_\mathbf{0}^{\mathbf{32}} & \mathbf{S}_\mathbf{0}^{\mathbf{33}} \end{pmatrix} \begin{pmatrix} \varphi_1 \\ \varphi_2 \\ \varphi_3 \end{pmatrix} = \begin{pmatrix} f_1 \\ f_2 \\ f_3 \end{pmatrix},$$

for the components of $\boldsymbol{\varphi}$.

In the case of (2) $\big($ e.g. the fiber is aligned to the $z$–axis and $\boldsymbol{f} = (f_1, 0, 0)\big)$, the off–diagonal blocks $\mathbf{S}_\mathbf{0}^{\mathbf{12}}, \mathbf{S}_\mathbf{0}^{\mathbf{13}}, \mathbf{S}_\mathbf{0}^{\mathbf{21}}, \mathbf{S}_\mathbf{0}^{\mathbf{23}}, \mathbf{S}_\mathbf{0}^{\mathbf{31}}, \mathbf{S}_\mathbf{0}^{\mathbf{33}}$ of the matrix $\mathbf{C} + \mathbf{S}_\mathbf{0}^{\text{full}}$ drop out, and we obtain the familiar discretization $(c\mathbf{I} + \mathbf{S_0})\varphi_1 = f_1$, yielding the only force component in $x$–direction.

*Remark* 3. Usually the matrix $\mathbf{C} + \mathbf{S}_\mathbf{0}^{\text{full}}$ is a *full* and *non–symmetric* matrix of dimension $(3n)^2$. If the fiber lies in a plane, i.e. if the torsion of the centerline vanishes, and if the right hand side $\boldsymbol{f}$ has also only components in this plane, then the local coordinate system spanned by the tangent $\boldsymbol{e_t}$ and the normal $\boldsymbol{e_n}$ of the fiber shall be used. In this situation, the binormal vector $\boldsymbol{e_b}$ is constant along the fiber. Using the decomposition of $\boldsymbol{\varphi}$ and $\boldsymbol{f}$ in the tangential and normal component, we obtain a reduced system of dimension $(2n)^2$.

## 8. Circular Arc in Translational Flow

In [2], Cox considers the force acting on an ellipsoid with minor axis $a$, bent to a circular arc between the angles $\theta_0$ and $\theta_1$. The free–stream velocity is $\boldsymbol{u_\infty} = \boldsymbol{e_1}$, see Figure 2. Cox gives an expression for the force acting on this body as an expansion in terms of $1/\ln a$. In [10], Johnson considers the same situation. He gives an approximative solution, obtained from an iteration procedure applied to an integral equation similar to (15). Using a discretization with $n = 400$ collocation points, minor axis $a = 10^{-4}$ and the angles $\theta_0 = 20°$ and $\theta_1 = 130°$, the resulting force, based on equation (15) is computed numerically. Figure 3 shows the results. Good agreement is found between Johnson's approximation and the numerical solution. The result, published by Cox, is in less agreement, especially near to the ends of the fiber. A reason for this might be an inaccurate treatment of the fiber shape at the ends.

## 9. Conclusion

The integral equations arising from flow past slender fibers are numerically solved by a collocation method. In the case of a straight fiber the collocation scheme exactly recovers the eigenvalues and the eigenvectors converge to the eigenfunctions of the continuous operator.

The collocation scheme is applied to fibers with arbitrary centerlines. A treatment of the integral equations arising from the slender–body approximations of Oseen's equation is seemingly possible.

## References

1. S. T. Chung and T. H. Kwon, *Numerical simulation of fiber orientation in injection moulding of short–fiber–reinforced thermoplastics*, Polymer Engineering and Science **7** (1995), no. 35, 604–618.

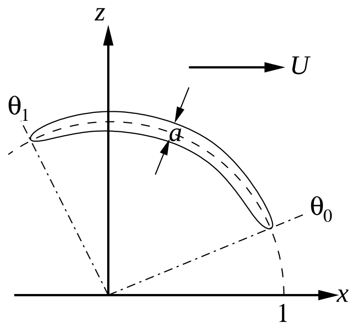


FIGURE 2. Sketch of the test case in Cox [2]. The fiber has an ellipsoidal shape with minor axis $a$ and is bent to a circular arc between $\theta_0$ and $\theta_1$. The direction of the free flow is $\boldsymbol{e_1}$.

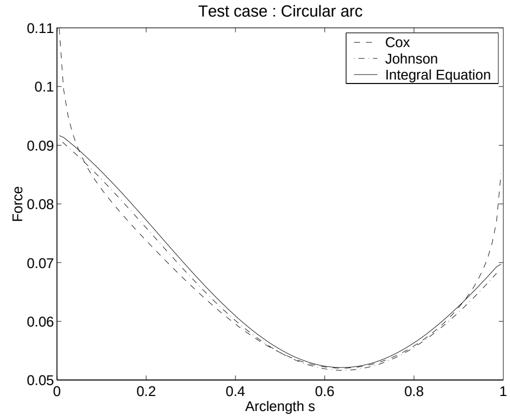


FIGURE 3. Force in $x$–direction for an ellipsoid bent to a circular arc between $\theta_0 = 20°$ and $\theta_1 = 130°$. Results due to Cox [2] ('– –'), Johnson [10] ('– .') and the numerical solution of the integral equation (15) ('—'). The minor axis of the ellipsoid is taken to be $a = 10^{-4}$.


2. R. G. Cox, *The motion of long slender bodies in a viscous fluid. Part 1. General theory*, Journal of Fluid Mechanics **44** (1970), no. 4, 791–810.
3. S. M. Dinh and R. C. Armstrong, *A rheological equation of state for semiconcentrated fiber suspensions*, Journal of Rheology **3** (1984), no. 28, 207–227.
4. X. Fan, N. Phan-Thien, and R. Zheng, *A direct simulation of fibre suspensions*, J. Non–Newtonian Fluid Mech. **74** (1998), 113–135.
5. T. Götz, *Interactions of fibers and flow : Asymptotics, theory and numerics*, Ph.D. thesis, University of Kaiserslautern, Germany, submitted 2000.
6. T. Götz and A. Unterreiter, *On an integral equation model for slender bodies in low–Reynolds–number flows*, Berichte der Arbeitsgruppe Technomathematik 219, University of Kaiserslautern, 1999.
7. ———, *Analysis and numerics of an integral equation model for slender bodies in low–Reynolds–number flows*, Journal of Integral Equations and Applications to appear **12** (2000), no. 3.
8. I. S. Gradshtyn and I. M. Rhyzik, *Table of integrals, series and products*, Academic Press, 1973.
9. W. Hackbusch, *Integralgleichungen : Theorie und Numerik*, Teubner, 1989.
10. R. E. Johnson, *An improved slender–body theory for Stokes flow*, Journal of Fluid Mechanics **99** (1980), no. 2, 411–431.
11. J. B. Keller and S. I. Rubinow, *Slender–body theory for slow viscous flow*, Journal of Fluid Mechanics **75** (1976), no. 4, 705–714.
12. T. Kida and T. Take, *Integral approach of asymptotic expansions for low–Reynolds–number flow past an arbitrary cylinder*, JSME International Journal, Series II **35** (1992), no. 2, 138–143.
13. J. Lighthill, *Mathematical biofluiddynamics*, SIAM, 1975.
14. H. Ockendon and E. L. Terril, *A mathematical model for the wet–spinning process*, Euro. J. Appl. Math. **4** (1993), 341–360.
15. H. Power, *Matched–asymptotic analysis of low–Reynolds number flow past a cylinder of arbitrary cross–sectional shape*, Math. Aplic. Comp. **9** (1990), no. 2, 111–122.
16. R. Schaback and H. Werner, *Praktische Mathematik*, Springer, 1992.
17. M. Shelley and T. Ueda, *The Stoksian Hydrodynamics of Flexing, Stretching Filaments*, `http://math.nyu.edu/faculty/shelley/heleshaw/Bubble.htm`, to appear in Physica D (1999).


DEPT. OF MATHEMATICS, UNIVERSITY OF KAISERSLAUTERN, D–67663 KAISERSLAUTERN
*E-mail address*: `goetz@mathematik.uni-kl.de`